J. Membrane Biol. 81, 113–125 (1984)

The Journal of
Membrane Biology

Current-Voltage Characteristics of the Proton Pump at *Chara* Plasmalemma: I. pH Dependence

M.J. Beilby
Botany School, University of Cambridge, Cambridge, England

Summary. A feature of the current-voltage (*I/V*) and conductance-voltage (*G/V*) characteristics is described, which can be attributed to the action of the proton pump at the *Chara* plasmalemma. The study of pH dependence in the range 4.5 to 11.0 and exposure to metabolic inhibitors confirm the pump involvement.

A model describing kinetics of H^+-extruding ATPase (Hansen, U.-P., Gradmann, D., Sanders, D., Slayman, C.L. 1981. *J. Membrane Biol.* **63**:165–190) is fitted to the data yielding the *I/V* and *G/V* relationships of the *Chara* proton pump. The results show that the stoichiometry is $1H^+ : 1ATP$.

Key Words proton pump · current-voltage characteristics · conductance · pH dependence · inhibitors · kinetic model

Introduction

A proton-extruding ATPase has been isolated from the *Neurospora* membrane (e.g., Scarborough, 1976), but only indirect indication of its existence can be furnished for the *Chara* plasmalemma. This circumstantial evidence, however, is plentiful. For pH_o greater than 6.0 the transmembrane PD is more hyperpolarized than explicable by the concentration gradients of the ions present and is diminished by the application of metabolic inhibitors (e.g., Spanswick, 1972, 1974; Richards & Hope, 1974). Measurements of the cytoplasmic pH (Walker & Smith, 1975; Spanswick & Miller, 1977*a*) give a high value (~7.5), out of equilibrium at any pH_o. In a stagnant medium acidification occurs (e.g., Spear, Barr & Barr, 1969). ATP is necessary both for the hyperpolarized state (Shimmen & Tazawa, 1977) and for the proton extrusion (Shimmen & Tazawa, 1980).

No consensus has been reached about the *Chara* proton pump stoichiometry, the current-voltage (*I/V*) characteristics and the contribution to the total conductance. Some experiments with inhibitors indicate that most of the membrane conductance is due to the pump (e.g., Keifer & Spanswick, 1978), while others suggest that the pump provides only a small contribution (Richards & Hope, 1974). Kishimoto, Kami-Ike and Takeuchi (1980) estimate the pump conductance to be slightly more than a half of the total. The conductance obtained from the electrical measurements greatly exceeds that calculated from the tracer experiments (e.g., Hope & Walker, 1975). This discrepancy is often attributed to the pump and the passive H^+ fluxes. A novel approach has been adopted by Smith and Beilby (1983), who observed a decrease in the resting conductance following an action potential. They postulated that this effect is caused by a transient inhibition of the proton pump. If this inhibition is complete, then the contribution of the pump to the total membrane conductance does not amount to more than 20 to 30%.

A central maximum was discovered in the *I/V* characteristics of *Chara* plasmalemma (Beilby & Beilby, 1983). By fitting the Hansen, Gradmann, Sanders and Slayman model (1981), which predicts such a feature, a new insight was gained into the proton pump kinetics. The approach yields the *I/V* and *G/V* characteristics and the stoichiometry of the *Chara* proton pump.

Materials and Methods

Young leaf cells of *Chara corallina* were used. These were kept in the standard APW (0.1 mM KCl, 1.0 mM NaCl, 0.5 mM $CaCl_2$, 1.0 mM HEPES, NaOH to adjust to pH 7.5, 0.47 mM) at least a day prior to the experiment.

The apparatus has been described in detail (Beilby & Beilby, 1983). The clamp circuit accepted commands from MINC 11 computer, which also data-logged both the membrane potential and the clamp current. To furnish an *I/V* curve the cell was clamped to a bipolar staircase with pulses of 20 to 40 msec wide. This interval allowed sufficient time for the clamp current to come to equilibrium. The potential and current were sampled every 2 msec. A polynomial was fitted to the data and differenti-

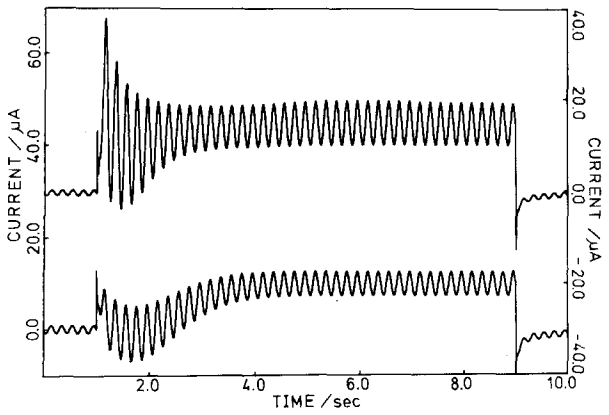

Fig. 1. A comparison between the clamp current flowing across plasmalemma (upper trace, right-hand vertical axis) and plasmalemma and tonoplast in series (lower trace, left-hand vertical axis). For the first sec the potential is clamped at the resting level, then to 0 for 8 sec and finally back to the resting level. The linear clamp command is modulated by 20 mV, 5 Hz sinusoidal signal to monitor the conductance. The conductance is given by (I_o/V_o) cos ϕ, where I_o and V_o are the amplitudes of the current and potential sine waves, respectively, and ϕ is the phase angle, which can be neglected at depolarized levels (Beilby & Beilby, 1983). Note particularly the large conductance increase of the plasmalemma, as the potential level is depolarized

ated to obtain the *G/V* characteristics (*see* Fig. 4*b* and *c*). AC conductance was also measured by superimposing a small sinusoidal signal (10–20 mV) with frequency of 5 Hz on a linear clamp command (*see also* Beilby & Beilby, 1983).

The cells were placed in the chamber and illuminated by fiber optics source Intralux H150 Volpi, light intensity of 50–100 μeinsteins/m^2 sec (~10–20 W/m^2, when the light frequency was approximated as the middle of the visible spectrum). The *I/V* characteristics were monitored until stabilization was reached (up to 2 hr in some cells).

To ensure that the potential-measuring electrode was in the cytoplasm, the cell was clamped at 0. At this potential the behavior of the plasmalemma and the two membranes in series is quite distinct (*see* Fig. 1). At the resting potential the resistance of the tonoplast is ~4 times lower than that of the plasmalemma, and thus the combination is dominated by the properties of the latter (Coster & Smith, 1977). At the time of excitation, however, the resistance of the plasmalemma seems to drop below that of the tonoplast—thus with the electrode in the cytoplasm the changes in conductance (as reflected by the amplitude of the clamp-current sine wave in Fig. 1) are more marked. When both membranes in series are clamped, the tonoplast conductance becomes visible at the peak of excitation. Our measurements of the tonoplast slope conductance are ~20 S m^{-2} (*see* Fig. 2 insert), rather a large value compared to those measured by Findlay and Hope (1964) and Coster and Smith (1977).

The *I/V* curves for the plasmalemma and for both membranes in series are shown in Fig. 2. As the cell was in the resting state while the *I/V* data were gathered, the two membranes in series reflected mainly the properties of the plasmalemma. The *I/V* curve for the membranes in series was shifted by ~20 mV (the PD across the tonoplast) in the depolarizing direction. To isolate the *I/V* characteristics of the two series elements, the PD across plasmalemma was subtracted from the PD across both membranes, when the currents were the same. (Both sets of data were collected within 30 min, so that changes in either membrane were unlikely.) A limited *I/V* curve for the tonoplast was thus obtained (*see* inset in Fig. 2).

When the cells were made inexcitable by La^{3+} or DES, it was no longer possible to be absolutely sure of the potential-measuring electrode position. While the attempt was made to keep the electrode in the cytoplasm at all times, a failure to do so should not significantly affect the results.

To change the pH of the APW, 1 mM zwitterionic buffers were used: MES, pH 4.5–6.5; HEPES, pH 7.5; TAPS, pH 8.5–9.5; CAPS, pH 10–11. NaOH was employed to adjust the pH to a desired value. Solutions were freshly made up before the experiments, and the flow rate through the chamber was high.

The cell was kept in APW of pH 7.5 between pH_o changes. The time in APW of other pH_o values was minimized (~20 min) to prevent fluctuations of the cytoplasmic pH. Upon a pH_o change (except for pH_o above 9.0, which will be discussed elsewhere) the potential stabilized within ~10 min and the *I/V* curves were reproducible after this time.

To obtain *I/V* curves over a wider potential range, excitation was removed. La^{3+} was chosen as an excitation-blocking agent, because its action was complete, relatively fast and irreversible in APW. Keifer and Spanswick (1978, 1979) found that 0.5 mM $LaCl_3$ depolarized the resting potential by ~70 mV, but caused no change in the membrane conductance or ATP concentration. In my experiments, 0.1 mM $LaCl_3$ was sufficient to remove excitation. At this concentration the resting PD depolarized by only 10 to 20 mV. After ~2 hr the cell was tested for excitability and, if this was absent, returned into APW. (An example of a clamp current before and after application of La^{3+} can be seen in Fig. 3.) The cells then hyperpolarized to potentials equal or *more negative* than before La^{3+} application. At pH_o 7.5, where the effect of $LaCl_3$ was at first tested, both the shape of the *I/V* curve and the *G*-maximum were essentially unchanged (*compare* Figs. 4*a*, *c* and 6*a*, *b*).

DES (diethyl stilbestrol) has been found to be an effective inhibitor of membrane-bound ATPases, both by direct action and by interference with oxidative phosphorylation, thus reducing the supply of ATP (Balke & Hodges, 1977, Keifer & Spanswick, 1979). The stock solution of 40 mM DES in ethanol was prepared freshly before an experiment or stored at 4°C for no more than three days. The addition of ethanol alone to APW in comparable concentrations had no effect on the cell behavior (M.J. Beilby, *unpublished data*). Our cells seemed more sensitive to DES, and the concentration was lowered from 40 μM (Keifer & Spanswick, 1979; Keifer & Lucas, 1982) to 10 μM. Cells were also exposed to 2 mM NaN_3. To test the effect of CO_2, 2 mM $NaHCO_3$ was added at pH_o 5.0.

Results

I/V and G/V Curves as Function of pH_o in Excitable Cells

The *I/V* characteristics in the pH_o range 4.5 to 8.5 can be seen in Fig. 4*a*. The potential range was delimited by the punchthrough at the hyperpolarized potentials and by the excitation transients at ~−100 mV. As pH_o decreased, the punchthrough

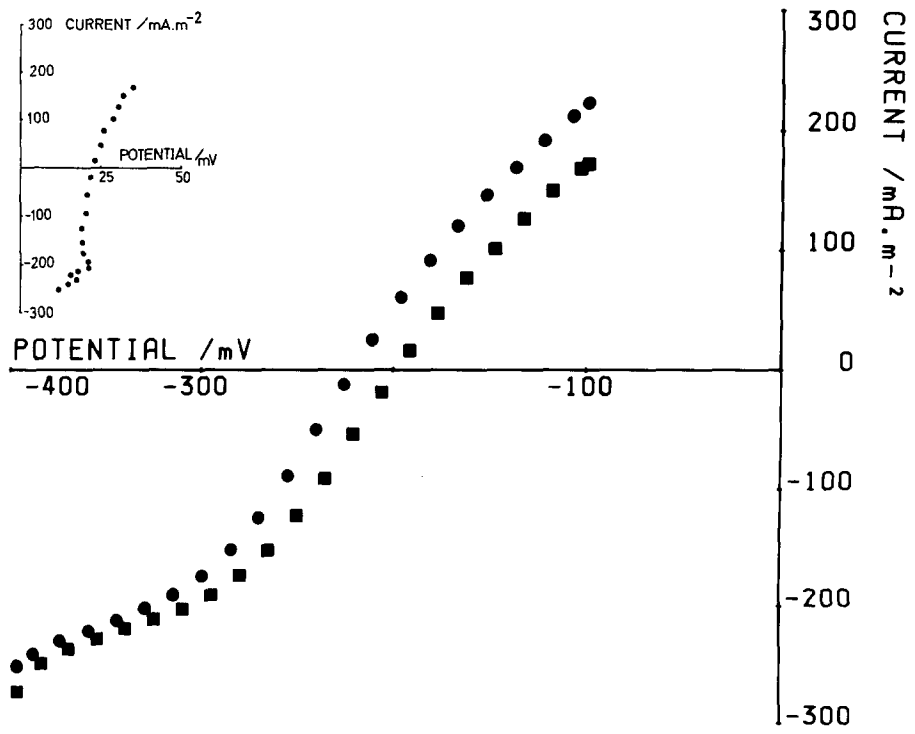

Fig. 2. The *I/V* characteristics of the plasmalemma (●) and both membranes in series (■). The potentials can be subtracted when the current is the same in each case, giving a limited *I/V* curve for the tonoplast, as shown in the inset

potential became more depolarized as observed by Coster (1969). At pH_o 4.5 the threshold for excitation shifted to more depolarized level (Beilby, 1977) and the potential range was extended to −70 mV. Figure 4*b* shows the polynomials fitted to the above data. The differentials of these give the *G/V* curves in Fig. 4*c*.

At pH_o above 9.0 the pump conductance became progressively swamped by the increasing H^+ conductance (*see* Fig. 5) as the cells were entering the 'Bisson' state (e.g., Bisson & Walker, 1981). However, the conductance maximum was still distinguishable in the conductance profiles (Fig. 5*b*).

I/V and G/V Curves as Function of pH_o in La^{3+}-Deactivated Cells

The summary of the data is shown in Fig. 6. The data were treated as in Fig. 4. As the difference in *I/V* characteristics was small at pH_o 7.5 and 8.5, the pH_o range was truncated at 7.5. The treated cells seemed less sensitive to pH_o change than the excitable cells. Compare, for instance, the resting potentials.

The Effect of Inhibitors

DES caused a steady depolarization, which reached a stable level after ~30 min. In cells not treated with

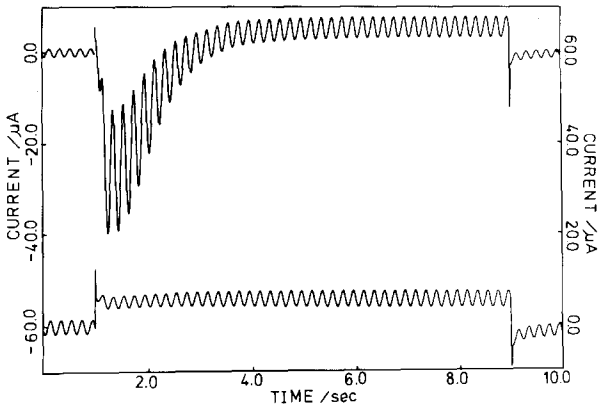

Fig. 3. The clamp currents at −80 mV before (upper trace, left-hand vertical axis) and after (lower trace, right-hand vertical axis) application of La^{3+}. Apart from the middle potential level, the clamping protocol is as in Fig. 1. Note that the conductance remains virtually unchanged upon the clamp level depolarization in the La^{3+}-treated cell

La^{3+} the resultant resting PD's were −60 to −100 mV, more positive than those observed by Keifer and Lucas (1982). Collected data from these cells can be seen in Fig. 7 (open points). A straight line could be fitted through the data.

After the DES was put on and the PD reached steady value, the *I/V* curve also stabilized. In one cell the pH_o was changed at this point in the range 4.5 to 7.5 with no appreciable effect on the shape of

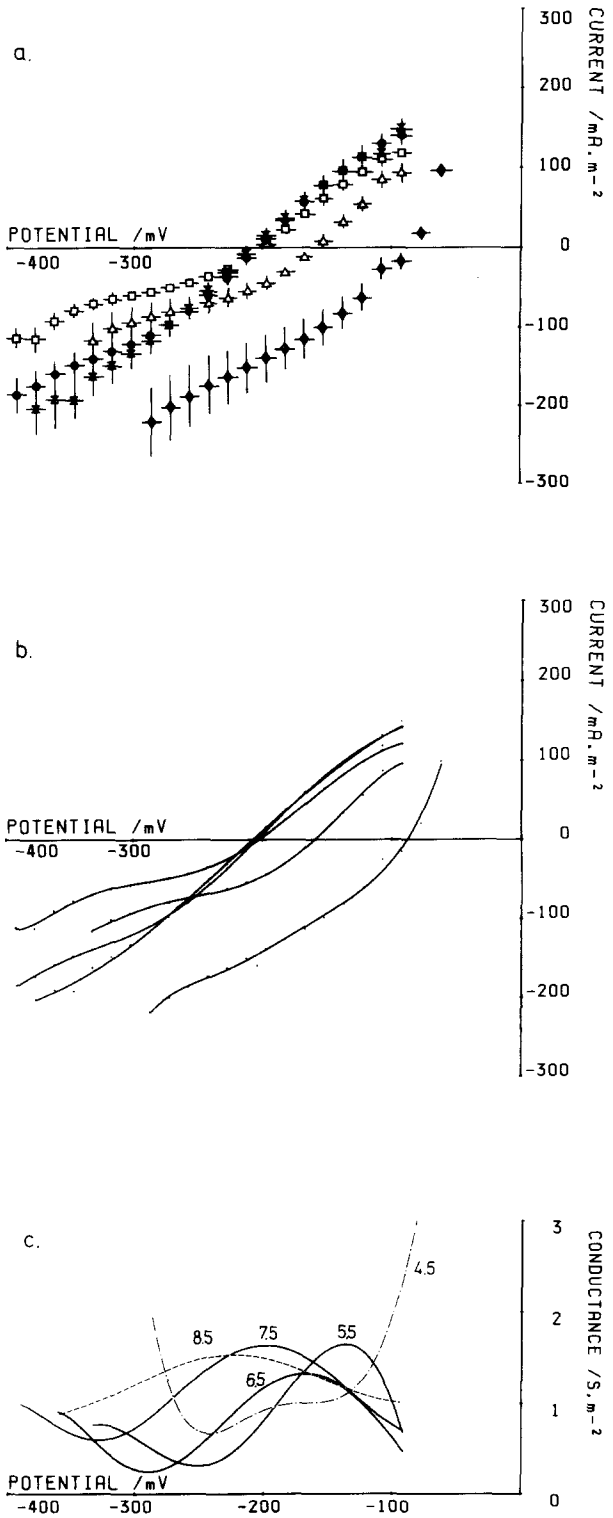

Fig. 4. (*a*): A summary of the *I/V* response of four cells to pH_o variation: ⧖, 8.5; ●, 7.5; □, 6.5; △, 5.5; ◆, 4.5. The horizontal bars denote the grouping of the data into intervals of 20 mV, the vertical bars are the standard error. (*b*): Polynomials fitted to the data of *a*, which are represented as points. (*c*): *G/V* characteristics obtained by differentiation of *b*. The values of pH_o are indicated next to each curve. The curves at pH_o 8.5 --- and 4.5 -·-·- are represented by broken lines for clarity

the *I/V* curve. Some cells recovered when returned to APW, but in some the potential would suddenly and irreversibly decline after a long exposure (several hours) to DES.

The cells became inexcitable in DES, and the conductance rose slowly when the clamp level was depolarized (*see* Fig. 8).

In the La^{3+}-treated cells, DES decreased the PD to a similar level (~−100 mV). The *I/V* curves continued to change, however, after the resting PD stabilized (Fig. 7, filled symbols). A more detailed history of the inhibition and partial recovery is shown in Fig. 9.

Sodium azide also caused depolarization, but not to such an extent as DES. In 2 mM azide, the resting PD declined after some hours, but sometimes would show a spontaneous recovery. The conductance decreased (Fig. 10 insert).

In darkness (or rather very dim light, as the light-proofing was not complete), the cells depolarized only by 10–20 mV, but the conductance maximum flattened considerably (Fig. 11). The conductance profile was restored to previous value after 30 min of light.

The *I/V* and *G/V* characteristics were totally insensitive to presence of CO_2 in contrast to behavior of *Nitella* (Spanswick & Miller, 1977*b*).

In APW with Cl^- replaced by $SO_4^=$ the *I/V* and *G/V* profiles tend to remain unchanged, but in some cells the conductance maximum flattened.

Discussion

The nonlinear nature of the *I/V* curves (Figs. 4*a*, 5*a*, and 6*a*) might seem contrary to the bulk of the literature on the subject. However, linear *I/V* characteristics have been observed in the past probably because the potential range was too small (−100 to −300 mV), the current was not evenly distributed over the cell area (point clamping), and the data-logging procedures were inadequate. Our techniques avoid these problems, and the bipolar staircase method minimizes transport number effects. Further, the existence of the *G*-maximum was confirmed by impedance measurements, a method independent of the *I/V* analysis (Beilby & Beilby, 1983).

Let us consider the processes occurring at the plasmalemma and their contribution to the *I/V* and *G/V* characteristics of the membrane (*see* a schematic diagram on Fig. 12). The Double Fixed Charge Membrane (DFCM) theory constructs a mathematical model of two regions of opposite charge in contact with each other (Coster, 1965). It is now thought that this mechanism only becomes

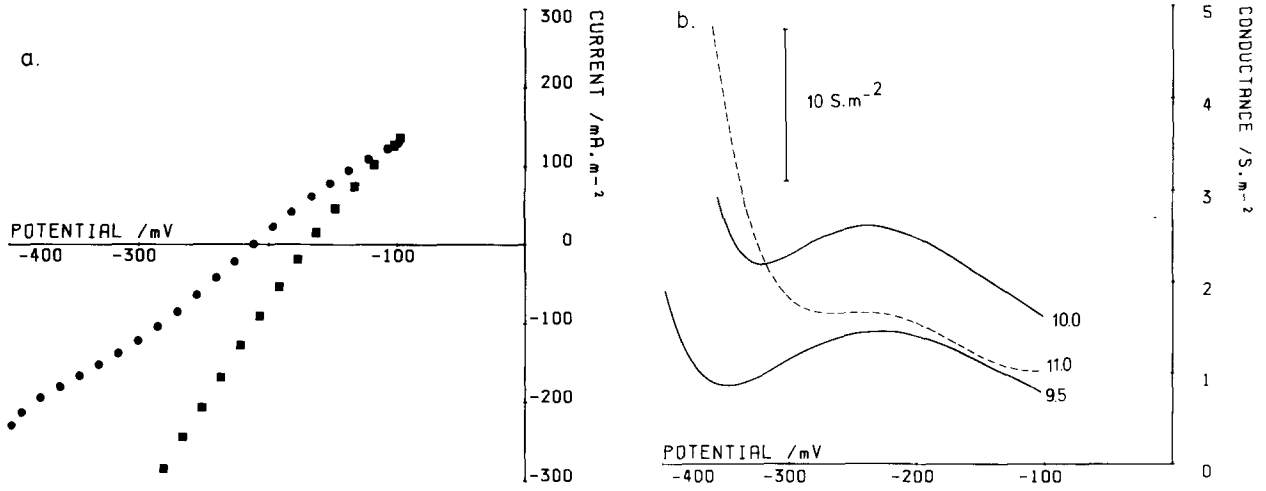

Fig. 5. (*a*): For completeness, the *I/V* curves at pH 9.5 (●) and 10.0 (■) are included. With the increasing pH_o the membrane is more permeable to H^+ and the Nernst potential for protons becomes more important in the determination of the transmembrane PD. (*b*): *G/V* curves obtained by differentiation of the polynomials from *a*. The pH_o is indicated next to each curve. The dashed curve was obtained by differentiation of a polynomial fitted to data at pH_o 11.0. The conductance scale for this record is given on the left-hand side. Note that the *G* maximum remains at −220 mV at the pH_o range 9.5 to 11.0

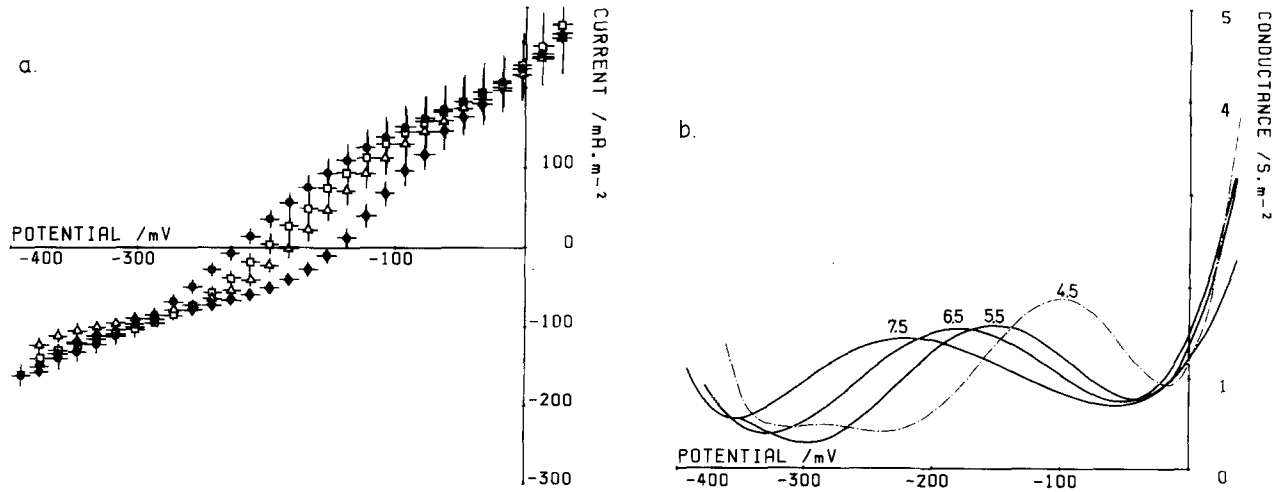

Fig. 6. (*a*): The La^{3+}-inactivated data, summary of four cells at a range of pH_o: ●, 7.5; □, 6.5; △, 5.5; ◆, 4.5; Data was treated as in Fig. 4. (*b*): as in Fig. 4*c*

important at extreme potentials and is responsible for the rectification and punchthrough. There is a growing body of evidence for the existence of gated K^+ channels analogous to those in the nerve (Keifer & Lucas, 1982; M.A. Bisson, *private communication*). The voltage dependence is not known and the equilibrium potential in APW is estimated at ~−160 mV. A leakage current due to K^+, Na^+ and possibly H^+ may also exist. The voltage dependence is again not known and the diffusion potential is estimated between −120 and −160 mV. Above pH_o 10.5 the resting PD follows E_H as the membrane becomes permeable to H^+ or OH^- (Bisson & Walker, 1981). This pathway is not included in Fig. 12, as most of the data discussed in this communication were obtained at pH_o below 9.0. The H^+-extruding ATPase is thought to be responsible for the hyperpolarized state of the *Chara* PD. The thermodynamic considerations, possible after the measurement of the cytoplasmic pH (Walker & Smith, 1975), yield a good agreement between the observed resting PD's and the equilibrium (E_p) calculated for a range of pH_o

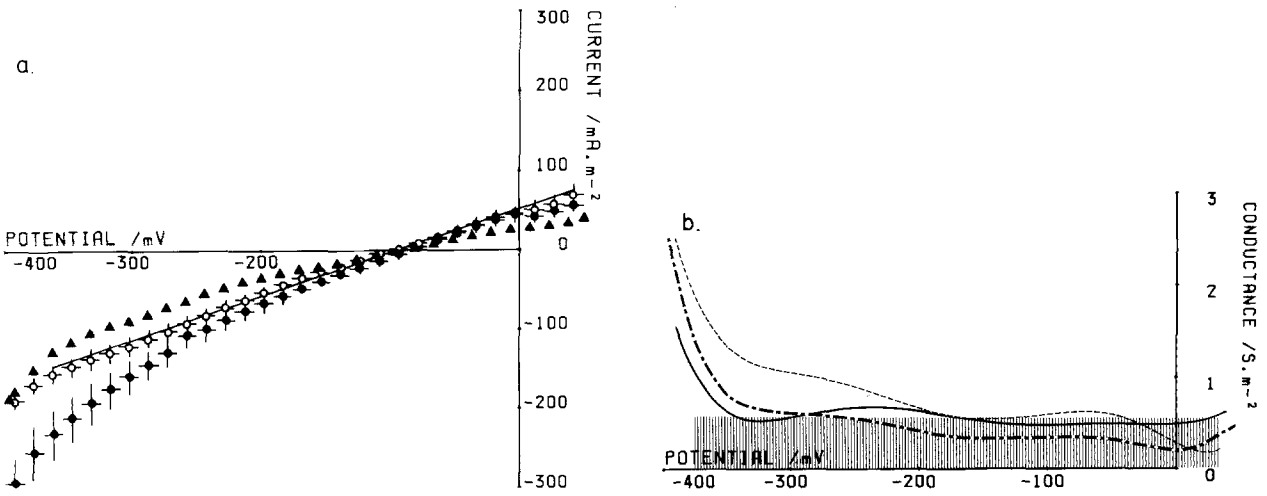

Fig. 7. (*a*): The effect of DES. Ten *I/V* runs are summarized from nine normal cells (○). Data are treated as in Figs. 4 and 6. A straight line was fitted by sight. Four La^{3+}-treated cells exposed to DES for 30 min (●). A single *I/V* run on La^{3+}-treated cell, with DES exposure of 1 hr 15 min (▲). (*b*): *G/V* characteristics obtained from polynomials of the best fit; La^{3+}-treated cell statistics ---, single run -.-.-, normal cell statistics ——. The shaded region indicates the conductance due to the fitted straight line in *a*

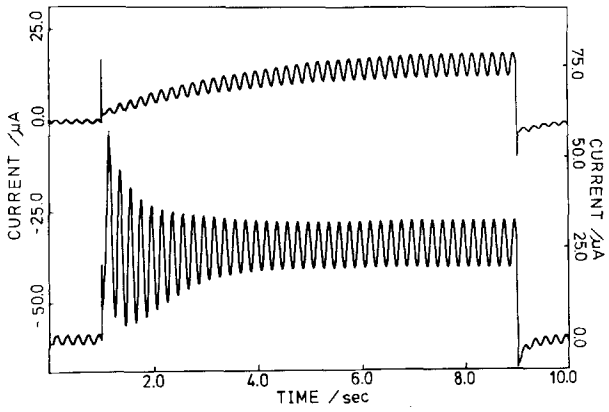

Fig. 8. Clamp current after the cell was exposed to DES for 1 hr 20 min (upper trace, left-hand vertical axis). The clamp commands were as in Fig. 1. Note the slow *G*-rise (~5 sec) after the clamp level depolarized. A clamp current at the beginning of the experiment (same clamp commands) is included for comparison (lower trace, right-hand vertical axis)

with the stoichiometry $2H^+$/ATP and the pump stalled (e.g., Smith & Walker, 1981). By modelling the membrane as a circuit with parallel arms containing the passive and the pump electromotive forces and conductances, Kishimoto et al. (1980) found a similar equilibrium potential (between −240 and −280 mV at pH_o 7.0) under normal conditions. Following an application of inhibitors, the calculated E_p would swing to ~−400 mV before declining, a PD in excess of that predicted by the thermodynamic calculations. Later, Walker (1981) showed that this hyperpolarization could be an artifact of the calculation process. However, large PD's were measured by Bisson and Walker (1982) and Lucas (1982) under various conditions. Thus the value of E_p is uncertain.

The conductance maximum occurs well below any equilibrium potential of the above processes, apart from the proton pump. Further, the conductance maximum moves with a change in pH_o. If this feature is due to the proton pump, then its contribution to the resting conductance is more than $\frac{3}{4}$ of the total in the pH_o range 4.5 to 7.5. (Consider, for instance, the Fig. 10 insert.)

After the application of DES to excitable cells, a linear *I/V* relationship is obtained, giving perhaps the leakage conductance. There are differences in the way the La^{3+}-treated cells and the normal cells respond to pH_o change and DES inhibition (*see* Figs. 4, 6, 7 and 9). Keifer and Spanswick (1978) found that $LaCl_3$ greatly reduced the membrane permeability to K^+, P_K. They also noted that P_K decreased as pH_o changed from 8 to 5. If the *I/V* curve between ~−300 and −50 mV (before punch-through or rectification set in) is viewed as a juxtaposition of a linear leak (mainly due to K^+) and nonlinear pump characteristics, then smaller P_K would manifest itself by decreasing the overall slope of the *I/V* curve. This is, indeed, observed for normal cells at pH_o 6.5 and 5.5. However, at pH_o 4.5 the overall slope increases. Keifer and Spanswick (1978) give no data for this pH_o, but Richards and Hope (1974) show a slight increase in P_K at pH_o 4. In La^{3+}-treated cells P_K is much lower

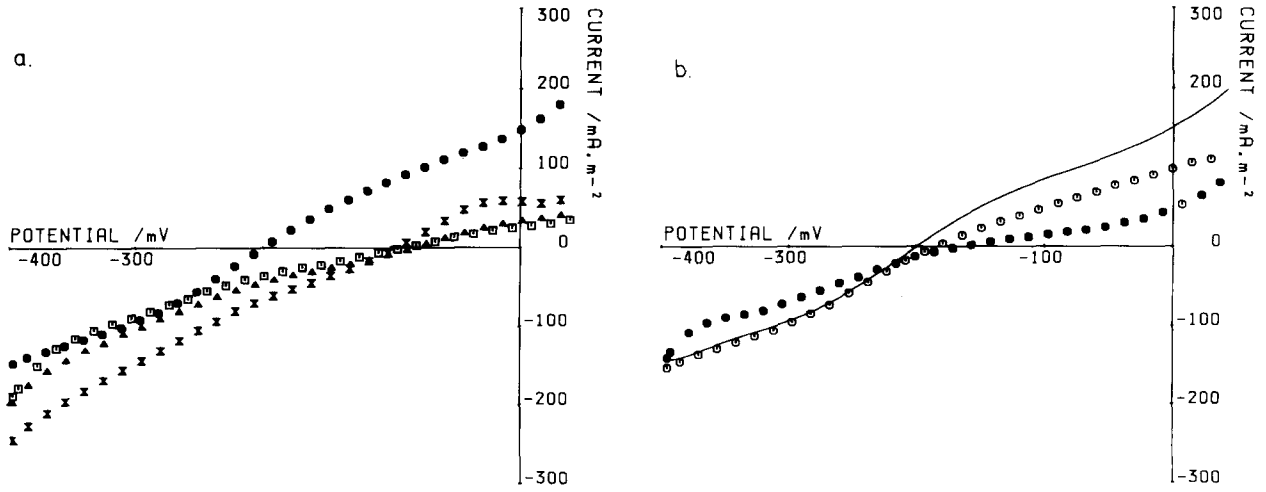

Fig. 9. (*a*): A history of inhibition by DES in La^{3+}-treated cell: ●, DES just put on; ⧗, 30 min (*compare* with the statistics in Fig. 7, filled circles); ▲, 1 hr; □, 1 hr 15 min; (*b*): Recovery after the cell was returned to APW: ●, 20 min wash out; ⓘ, 1 hr wash out; —, Pre-DES *I/V* curve

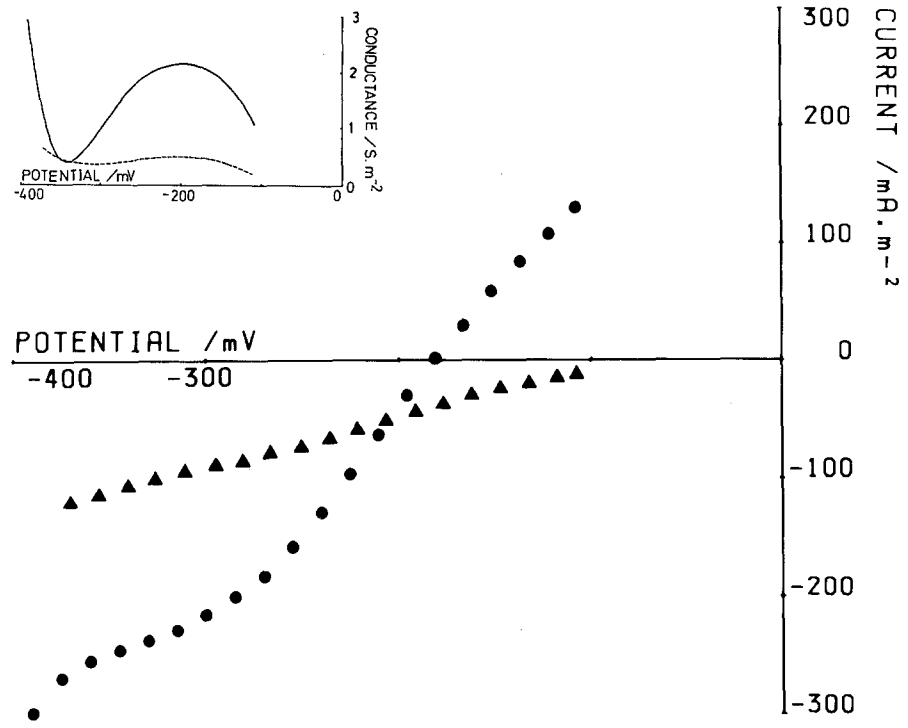

Fig. 10. *I/V* characteristics before (●) and after (▲) the cell was treated with 2 mM sodium azide. *Inset: G/V* characteristics in APW —— and 2 mM azide ----

and the variation with pH_o plays smaller part in the *I/V* characteristics. It is not clear at present why the La^{3+}-treated cells respond differently to DES.

The slow rising *G* in DES-treated cells (*see* Fig. 8) might be due to the K^+ channels opening in response to membrane PD change. This effect is normally obscured by the pump current and excitation. The slow *G* change was seen in both normal and La^{3+}-pretreated cells. The slow-rising current is not included in the *I/V* curve, because of the high speed of the staircase (*see* Materials and Methods and Beilby & Beilby, 1983). It will be interesting to obtain the voltage-dependence of this phenomenon by using the AC conductance measurements.

Keifer and Spanswick (1978) found that DES treatment reduced P_K. It is not clear at present

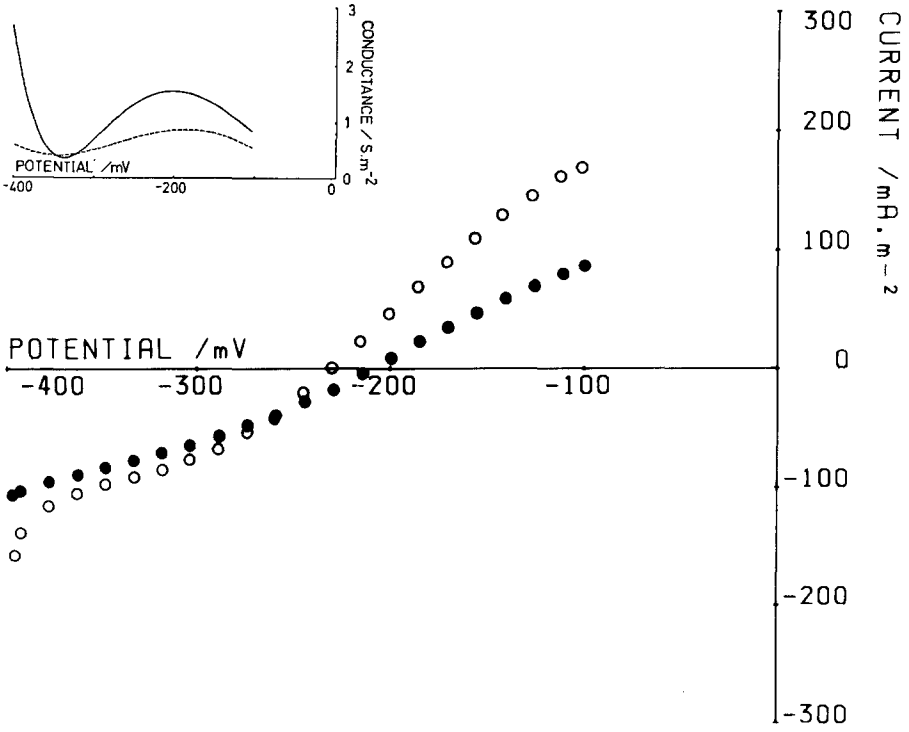

Fig. 11. *I/V* characteristics in light (○) and dark (●). *Inset: G/V* characteristics in light —— and dark ----

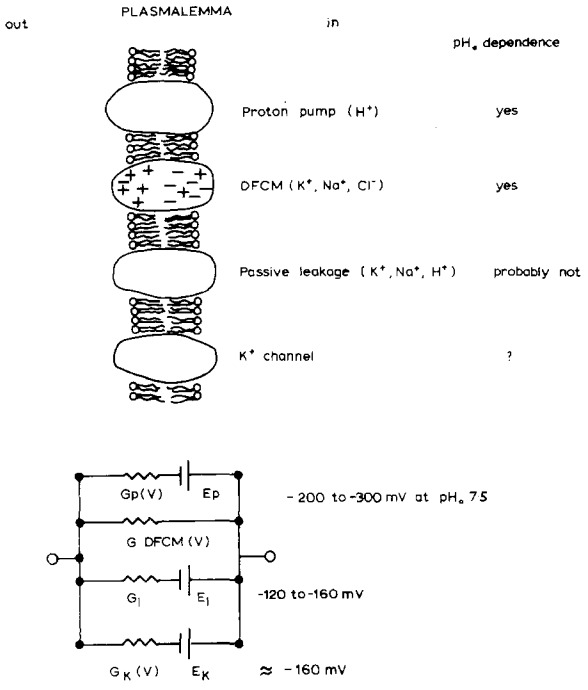

Fig. 12. A schematic diagram and a circuit representation of the transport processes at the plasmalemma involved in the *I/V* characteristics. This scheme is rather speculative. It is possible, for instance, that the leakage current is associated with the K^+ channel module

whether this effect is achieved via passive permeability, closing of the K^+ channels, or both. Smith and Walker (1981) discovered that the majority of K^+ channels open at potentials more depolarized than −150 mV. Thus as DES lowers the membrane potential, more K^+ channels would be expected to open than in the membrane hyperpolarized by electrogenesis. The DES *I/V* characteristics therefore represent some compromise between these effects.

Both the punchthrough and rectification were suppressed by the DES treatment. The reason for this is not clear. It is unlikely that these effects can be associated with the proton pump, as tracers have shown that the large currents at punchthrough consist of Cl^- (Coster & Hope, 1968), and K^+ outflow is thought to be responsible for the rectification.

It is interesting that the excitability is lost by the DES treatment. Shimmen and Tazawa (1977) found that ATP is essential for excitability in perfused cells. It is possible that ATP depletion due to DES in the intact cells (Keifer & Spanswick, 1979) may also lead to loss of excitation.

The inhibition of the proton pump in darkness is well documented in *Nitella* (Spanswick, 1972, 1974) and *Chara* (e.g., Tazawa, Fujii & Kikuyama, 1979). It is not understood, at present, why darkness has this inhibitory effect, as the ATP concentration is

not depleted (Keifer & Spanswick, 1979). It is interesting to note that while the resting conductance is almost halved in the dark, the resting PD became only slightly depolarized (*see* Fig. 11). The dark inhibition of the pump is incomplete or perhaps there are at least two aspects of the proton pump, which can be manipulated (G_p and E_p) (Spanswick, 1982).

As SO_4^- APW affects the membrane conductance only in some cells, it seems that the G maximum is independent of the $Cl^-/2H^+$ transport system (e.g., Beilby & Walker, 1981).

The temporary decrease in the membrane conductance following the action potential (Smith & Beilby, 1983) no longer seems to be due to the complete inhibition of the proton pump, as the conductance maximum in the G/V profile persists at the time of the G minimum (M.J. Beilby & J.R. Smith, *in preparation*).

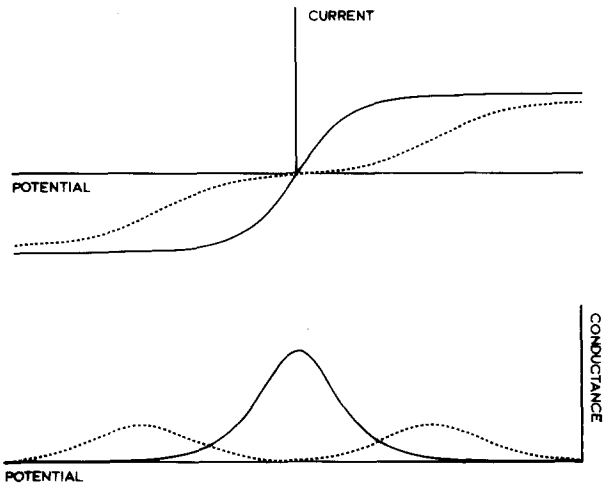

Fig. 13. The types of I/V and G/V curves generated by the Hansen et al. model. ——, $k^o_{io}[H^+]^z_i$ and $k^o_{oi}[H^+]^z_o > \kappa$'s; ----, $k^o_{io}[H^+]^z_i$ and $k^o_{oi}[H^+]^z_o < \kappa$'s. In this case $[H^+]^z_i = [H^+]^z_o$, $k^o_{io} = k^o_{oi}$ and $\kappa_{io} = \kappa_{oi}$ to obtain a symmetrical relationship

Modelling the Proton Pump Kinetics

Hansen et al. (1981) constructed a scheme for the kinetics of a H^+-extruding ATPase. They divided the process involved into the potential-dependent (via a symmetrical Eyring potential barrier, e.g., Lauger & Stark, 1970) with rate constants k_{io} and k_{oi} and potential-independent ones with rate constants κ_{oi} and κ_{io}. The I/V relationship for such a model is given by:

$$I = zFN \cdot \frac{\kappa_{oi}k^o_{io}\exp(zu/2) - \kappa_{io}k^o_{oi}\exp(-zu/2)}{k^o_{io}\exp(zu/2) + k^o_{oi}\exp(-zu/2) + \kappa_{io} + \kappa_{oi}} \quad (1)$$

N = number of carriers, z = pump stoichiometry, $u = FV/RT$ (with F, R and T having their usual meanings), $k_{io} = k^o_{io}\exp(zu/2)$; $k_{oi} = k^o_{oi}\exp(-zu/2)$.

The principal I/V and G/V (obtained by differentiating Eq. (1) with respect to potential) relationships arising from Eq. (1) are shown in Fig. 13. When k's are greater than κ's, the I/V relationship can be described essentially by the hyperbolic tangent function. The conductance yields a single maximum centered near the reversal potential. (The maximum is centered at the reversal potential if the I/V curve is symmetrical.) With κ's greater than k's the curve acquires more inflection points, producing two G maxima on each side of the reversal potential.

As the simplest possible model for a H^+-extruding ATPase contains five steps (Hansen et al., 1981), the meaning of the above parameters is obscured as various numbers of the carriers are sequestered in the different parts of the cycle. If changes in substrate level (for instance) are combined with the I/V analysis, it is desirable to develop the model further in such a form that the reactions that change during the experiment can be excluded from the lumped rate constants. Hansen et al. (1981) made such a modification, providing for a change in pH. This formulation requires a more complex model with four pairs of apparent rate constants, giving a range of possible properties. Some of this ambiguity can be removed by considering special mathematical cases and limiting conditions. One of such instances is where the PD and pH shift produce an equivalent response in the observed current. Such a behavior is, indeed, found in many systems (e.g., Schwab & Komor, 1978; Maloney & Schattschneider, 1980) including *Chara* (*see* Fig. 14). For such a system Eq. (1) becomes (Hansen et al., 1981):

$$I = zF\frac{N}{C} \cdot \frac{\kappa_{oi}k^o_{io}[H^+]^z_i\exp(zu/2) - \kappa_{io}k^o_{oi}[H^+]^z_o\exp(-zu/2)}{k^o_{io}[H^+]^z_i\exp(zu/2) + k^o_{oi}[H^+]^z_o\exp(-zu/2) + \kappa_{io} + \kappa_{oi}}. \quad (2)$$

To obtain the one maximum conductance profile of Fig. 13, $k^o_{io}[H^+]^z_i$ and $k^o_{oi}[H^+]^z_o$ must be greater than the κ's.

To fit the model to my data the I/V curves of Fig. 7 were subtracted from the data at various pH_o (Figs. 4 and 6). For the normal cells the average DES data were used (Fig. 7, open symbols). In the La^{3+}-treated cells, the single I/V run (Fig. 7, filled

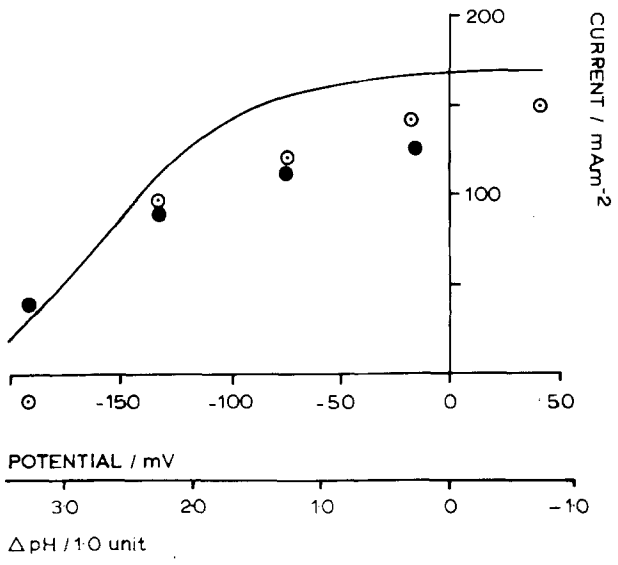

Fig. 14. Similar trends in the membrane current produced by the variation of the transmembrane PD or the pH difference. The electrochemical potential due to the pH difference, V_{pH}, was calculated as $2.3\frac{RT}{F}\Delta pH$, $\Delta pH = \log_{10}\frac{[H^+]_i}{[H^+]_o}$. The cytoplasmic pH was taken as 7.8, thus giving the most negative V_{pH} at pH_o 4.5 and most positive at pH_o 8.5. A family of I/V_{pH} curves could be plotted at various membrane potentials. The closest correspondence in overall shape between I/V and I/V_{pH} was obtained at $V = \sim -90$ mV for the normal cells (⊙) and ~ -120 mV for the La^{3+}-treated cells (●). These values are close to the reversal potentials of the leakage currents as seen in the DES data (Fig. 7). The continuous line is the I/V curve at pH_o 6.5 obtained from the model (*see* Fig. 15*b*)

triangles) was employed. It was only realized in the final experiments, that in these cells the I/V curve continues to change after the potential has stabilized. As the scatter in most of the data is small, I felt justified in taking such a shortcut. The resultant curves are shown as points in Fig. 15.

While the technique of obtaining the pump conductance by using metabolic inhibitors became widely accepted (e.g., Richards & Hope, 1974; Keifer & Spanswick, 1978; Keifer & Lucas, 1982), it must be viewed with caution. The inhibitors are usually not specific and are likely to interfere with several transport systems (e.g., DES seems to affect P_K, as mentioned earlier in the discussion). Further, in modelling the Na^+, K^+-ATPase Chapman, Johnson and Kootsey (1983) found that if ADP accumulates, while ATP supply is depleted, the pump becomes highly reversible, resulting in the difference I/V curves having no reversal potential. No data are available on concentration of ADP in plant cells while under influence of DES. Thus it is possible that difference I/V curves at pH_o 6.5 and 5.5 (Fig. 15*b* and *c*) suffer from such a problem. On the other hand, the I/V characteristics in DES-treated cells are almost linear (suggesting a leak conductance) and the difference I/V curves at pH_o 6.5 and 5.5 are similar in overall shape to the other difference curves. Neither of these aspects are observed in Chapman et al. (1983) calculations. It is more likely that the lack of reversal potential is caused by variation in the P_K with pH_o and due to DES treatment. The La^{3+} treatment diminishes the importance of P_K in the total I/V characteristics, giving "better" difference curves.

In view of these uncertainties, the work described in this communication can be seen only as a starting point. It will be necessary to compare the effects of a whole range of metabolic inhibitors, explore changes in $[K^+]_o$ and attempt other approaches to difference curves such as Gradmann, Hansen and Slayman (1982).

The model was fitted to the pH_o 7.5 data (Fig. 15*a*). The values of the parameters are given in the Table. The pH_o was then changed in the model (Fig. 16). Note how the simulated G profile changes with decreasing pH_o: the maximum moves in the depolarizing direction and becomes narrower and more pronounced in amplitude. Above pH_o 7.5 the two maxima conductance profile is obtained (the reversal PD is then close to -400 mV and the second maximum occurs at potentials below -400 mV). Effectively, this means that the right-hand G maximum does not change position with increasing pH_o above 7.5, only becomes slightly wider. The similarities between data in Figs. 4, 5 and 6 and the simulation (Fig. 16) are encouraging. Also note that at pH_o 11.0 the G maximum remains at ~ -200 mV (Fig. 5*b*). A direct comparison between the model and the data reveals some differences in the pH_o response, which means that some other rate constants change in response to the pH_o shift. The fit was adjusted and the changes are given in the Table. In the absence of further information, the significance of these variations is hard to interpret.

The stoichiometry of $z = 1$ was used. For $z > 1$ the s-curve was too steep to fit the data. The Hansen et al. model predicts very negative E_p values above pH_o 6.5 (*see* Fig. 16*a*). Such potentials have been observed by Lucas (1982). It does appear, therefore, that the pump is under kinetic rather than thermodynamic control. This is also suggested by the threshold concentration of ATP necessary for the activation of the pump (Spanswick, 1980).

For pH_o greater than 5.5 the pump current is close to saturation in the excitable region (Fig. 15) and is independent of PD changes above -100 mV. The approximation of the pump to an ideal current source, sometimes used in the transport lit-

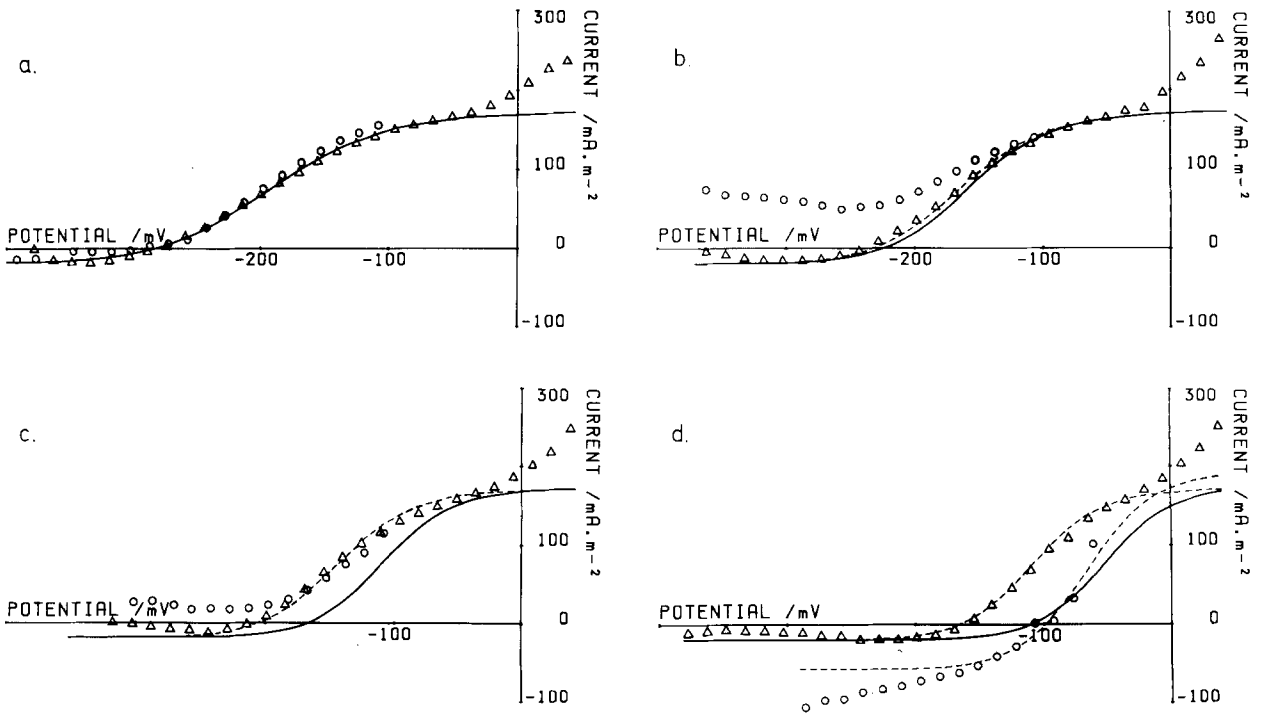

Fig. 15. (*a*): The *I/V* curves from Fig. 4 (○) and 6 (△) at pH_o 7.5 with the DES *I/V* curve subtracted (*see* text). The continuous line gives the calculated profile from the model. The parameters used are listed in the table. (*b*): As in *a* at pH_o 6.5. The normal cells data do not cross the potential axis (*see* discussion) and were not fitted. The continuous line was obtained from the model by changing pH_o only. The broken line represents a correction to the parameters to improve the fit (*see* the Table). (*c*): As in *b* at pH_o 5.5. (*d*): As in *b* at pH_o 4.5

Table.

pH_o	7.5	6.5	5.5	4.5	
	La^{3+} and normal cells	La^{3+} cells	La^{3+} cells	La^{3+} cells	Normal cells
k^o_{oi}	0.7×10^7	0.5×10^7	0.15×10^7	0.7×10^6	0.4×10^7
k^o_{io}	0.12×10^{12}	0.12×10^{12}	0.12×10^{12}	0.12×10^{12}	0.12×10^{12}
κ_{oi}	0.36×10^2	0.36×10^2	0.36×10^2	0.36×10^2	0.4×10^2
κ_{io}	4.5	4.5	4.5	4.5	0.12×10^2
N/C	0.5×10^{-7}	0.5×10^{-7}	0.5×10^{-7}	0.5×10^{-7}	0.5×10^{-7}

N/C is the number of carriers divided by a constant; for details *see* Hansen et al. (1981). The size of *N/C* is arbitrary. If the actual density differs, all rate constants will change in inverse proportion to *N/C*. The parameter values selected at pH_o 7.5 represent the optimal fit to the data, when only pH_o is changed in the model (shown by continuous lines in Fig. 15). Fits can be further improved by changing k^o_{oi} only in La^{3+}-treated cells and k^o_{oi}, κ_{oi} and κ_{io} in normal cells at pH_o 4.5.

erature, is justified in this instance. The pump conductance remains constant throughout the action potential, as predicted by Kishimoto et al. (1980).

Conclusions

The fitting of the Hansen et al. model reveals the *I/V* and the *G/V* characteristics and the stoichiometry (z = 1) of the *Chara* proton pump. In illuminated condition the pump constitutes the major contribution to the membrane conductance in pH_o range 7.5–4.5. The resting PD decline of the cell with pH_o decrease is thus not due to the inhibition of the pump, but due to the changes in the pump kinetics. It also appears that the pump remains operative in the high pH_o region (above pH_o 9.0), contrary to the scheme proposed by Bisson and Walker (1982).

The conductance maximum provides a new

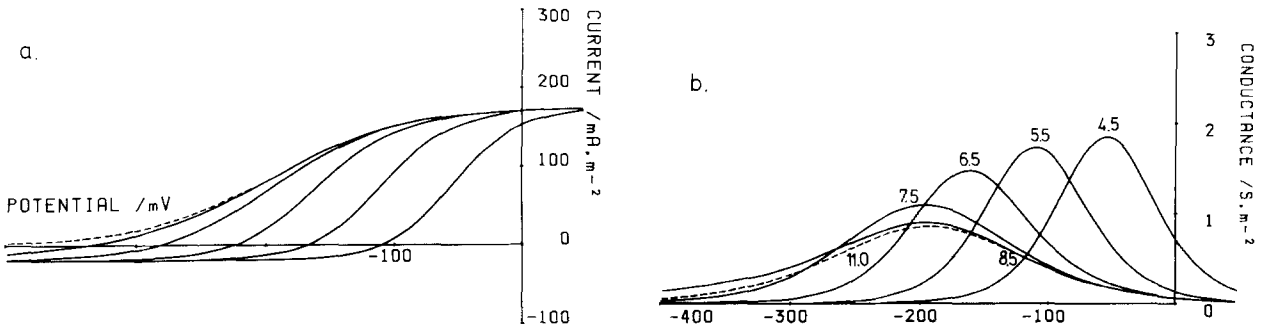

Fig. 16. The *I/V* (*a*) and *G/V* (*b*) curves in the pH_o range 4.5 to 11.0 obtained from the model with parameters fitted at pH_o 7.5 (*see* the Table). The profiles at pH_o 11.0 are shown as broken lines for clarity

way of testing whether the pump is operating in a given set of conditions. (That is, the presence of the maximum shows that the pump is on, while the reverse is not necessarily true. For instance, in darkness the hump flattens, but the large hyperpolarization indicates that the pump is still operating.) In the future this technique can be exploited to investigate the pump status in a range of K^+ concentrations and as a function of external Ca^{2+}.

This work was done with support from the Science and Engineering Research Council, which is gratefully acknowledged.

I would like to thank Dr. C.L. Slayman for drawing my attention to the kinetic pump model. I am also indebted to Dr. E.A.C. MacRobbie for critical reading of the manuscript and to my husband Bruce for mathematical assistance.

References

Balke, N.E., Hodges, T.K. 1977. Inhibition of ion absorption in oat roots: Comparison of diethylstilbestrol and oligomycin. *Plant Sci. Lett.* **10**:319–325

Beilby, M.J. 1977. An investigation into the electrochemical properties of cell membranes during excitation. Ph.D. Thesis, University of New South Wales, Sydney Australia

Beilby, M.J., Beilby, B.N. 1983. Potential dependence of the admittance of *Chara* plasmalemma. *J. Membrane Biol.* **74**:229–245

Beilby, M.J., Walker, N.A. 1981. Chloride transport in *Chara:* 1. Kinetics and current-voltage curves for a probable proton symport. *J. Exp. Bot.* **32**:43–54

Bisson, M.A., Walker, N.A. 1980. The *Chara* plasmalemma at high pH. Electrical measurements show rapid specific passive uniport of H^+ or OH^-. *J. Membrane Biol.* **56**:1–7

Bisson, M.A., Walker, N.A. 1981. The hyperpolarization of the *Chara* membrane at high pH: Effects of external potassium, internal pH, and DCCD. *J. Exp. Bot.* **32**:951–971

Bisson, M.A., Walker, N.A. 1982. Control of passive permeability in the *Chara* plasmalemma. *J. Exp. Bot.* **33**:520–532

Chapman, J.B., Johnson, E.A., Kootsey, J.M. 1983. Electrical and biochemical properties of an enzyme model of the sodium pump. *J. Membrane Biol.* **74**:139–153

Coster, H.G.L. 1965. A quantitative analysis of the voltage-current relationships of fixed charge membranes and the associated property of punchthrough. *Biophys. J.* **5**:669–86

Coster, H.G.L. 1969. The role of pH in the punchthrough effect in the electrical characteristics of *Chara australis*. *Aust. J. Biol. Sci.* **22**:365–374

Coster, H.G.L., Hope, A.B. 1968. Ionic relations of *Chara australis:* XI. Chloride fluxes. *Aust. J. Biol. Sci.* **21**:243–254

Coster, H.G.L., Smith, J.R. 1977. Low frequency impedance of *Chara corallina:* Simultaneous measurements of the separate plasmalemma and tonoplast capacitance and conductance. *Aust. J. Plant Physiol.* **4**:667–674

Findlay, G.P., Hope, A.B. 1964. Ionic relations of cells of *Chara australis:* VII. The separate electrical characteristics of the plasmalemma and tonoplast. *Aust. J. Biol. Sci.* **17**:62–77

Gradmann, D., Hansen, U.-P., Slayman, C.L. 1982. Reaction-kinetic analysis of current-voltage relationships for electrogenic pumps in *Neurospora* and *Acetabularia*. *Curr. Topics Membr. Transp.* **16**:257–276

Hansen, U.-P., Gradmann, D., Sanders, D., Slayman, C.L. 1981. Interpretation of current-voltage relationships for "active" ion transport systems: I. Steady-state reaction-kinetic analysis of class-I mechanisms. *J. Membrane Biol.* **63**:165–190

Hope, A.B., Walker, N.A. 1975. The physiology of giant algal cells. Cambridge University Press, London

Keifer, D.W., Lucas, W.J. 1982. Potassium channels in *Chara corallina*. Control and interaction with the electrogenic H^+ pump. *Plant Physiol.* **69**:781–788

Keifer, D.W., Spanswick, R.M. 1978. Activity of the electrogenic pump in *Chara corallina* as inferred from measurements of the membrane potential, conductance and potassium permeability. *Plant Physiol.* **62**:653–661

Keifer, D.W., Spanswick, R.M. 1979. Correlation of adenosine triphosphate levels in *Chara corallina* with the activity of the electrogenic pump. *Plant Physiol.* **64**:165–168

Kishimoto, U., Kami-Ike, N., Takeuchi, Y. 1980. The role of electrogenic pump in *Chara corallina*. *J. Membrane Biol.* **55**:149–156

Lauger, P., Stark, G. 1970. Kinetics of carrier-mediated ion transport across lipid bilayer membranes. *Biochim. Biophys. Acta* **211**:458–466

Lucas, W.J. 1982. Mechanism of acquisition of exogenous bicarbonate by internodal cells of *Chara corallina*. *Planta* **156**:181–192

Maloney, P.C., Schattschneider, S. 1980. Voltage sensitivity of proton-translocating adenosine 5′-triphosphate in *Streptococcus lactis*. *FEBS Lett.* **110**:337–340

Richards, J.L., Hope, A.B. 1974. The role of protons in determining membrane electrical characteristics in *Chara corallina*. *J. Membrane Biol.* **16**:121–144

Scarborough, G.A. 1976. The *Neurosopora* plasma membrane ATPase is an electrogenic pump. *Proc. Natl. Acad. Sci. USA* **73**:1485–1488

Schwab, W.G.W., Komor, E. 1978. A possible mechanistic role of the membrane potential in proton-sugar co-transport of *Chlorella*. *FEBS Lett.* **87**:157–160

Shimmen, T., Tazawa, M. 1977. Control of membrane potential and exitability of *Chara* cells with ATP and Mg^{2+}. *J. Membrane Biol.* **37**:167–186

Shimmen, T., Tazawa, M. 1980. Dependence of H^+ efflux on ATP in cells of *Chara australis*. *Plant Cell Physiol.* **21**:1007–1013

Smith, J.R., Beilby, M.J. 1983. Inhibition of electrogenic transport associated with the action potential in *Chara*. *J. Membrane Biol.* **71**:131–140

Smith, P.T., Walker, N.A. 1981. Studies on the perfused plasmalemma of *Chara corallina:* I. Current-voltage curves: ATP and potassium dependence. *J. Membrane Biol.* **60**:223–236

Spanswick, R.M. 1972. Evidence for an electrogenic ion pump in *Nitella translucens:* I. The effects of pH, K^+, Na^+, light and temperature on the membrane potential and resistance. *Biochim. Biophys. Acta* **288**:73–89

Spanswick, R.M. 1974. Evidence for an electrogenic ion pump in *Nitella translucens:* II. Control of the light-stimulated component of the membrane potential. *Biochim. Biophys. Acta* **332**:387–398

Spanswick, R.M. 1980. *In:* Plant Membrane Transport: Current Conceptual Issues. R.M. Spanswick, W.J. Lucas, and J. Dainty, editors. pp. 305–313. Elsevier, Amsterdam

Spanswick, R.M. 1982. The electrogenic pump in the plasma membrane of *Nitella*. *Curr. Topics Membr. Trans.* **16**:35–45

Spanswick, R.M., Miller, A.G. 1977*a*. Measurement of the cytoplasmic pH in *Nitella translucens*. *Plant Physiol.* **59**:664–666

Spanswick, R.M., Miller, A.G. 1977*b*. The effect of CO_2 on the Cl^- influx and electrogenic pump in *Nitella translucens*. *Colloq. Centre Natl. Rech. Sci. (Paris)* **258**:239–245

Spear, D.J., Barr, J.K., Barr, C.E. 1969. Localisation of hydrogen ion and chloride ion fluxes in *Nitella*. *J. Gen. Physiol.* **54**:397–414

Tazawa, M., Fujii, S., Kikuyama, M. 1979. Demonstration of light-induced potential change in *Chara* cells lacking tonoplast. *Plant Cell Physiol.* **20**:271–276

Walker, N.A., Smith, F.A. 1975. Intracellular pH in *Chara corallina* measured by DMO distribution. *Plant Sci. Lett.* **4**:125–132

Walker, N.A. 1981. Comments on "The Role of Electrogenic Pump in *Chara corallina*." *J. Membrane Biol.* **59**:151–152

Received 2 December 1983